Ultrafast transformation of graphite to diamond: An ab initio study of graphite under shock compression

Mundy, Christopher J ; Curioni, Alessandro ; Goldman, Nir ; Will Kuo, I-F ; Reed, Evan J ; Fried, Laurence E ; Ianuzzi, Marcella

Abstract: We report herein ab initio molecular dynamics simulations of graphite under shock compression in conjunction with the multiscale shock technique. Our simulations reveal that a novel short-lived layered diamond intermediate is formed within a few hundred of femtoseconds upon shock loading at a shock velocity of 12km/s (longitudinal stress>130 GPa), followed by formation of cubic diamond. The layered diamond state differs from the experimentally observed hexagonal diamond intermediate found at lower pressures and previous hydrostatic calculations in that a rapid buckling of the graphitic planes produces a mixture of hexagonal and cubic diamond (layered diamond). Direct calculation of the x-ray absorption spectra in our simulations reveals that the electronic structure of the final state closely resembles that of compressed cubic diamond.

DOI: https://doi.org/10.1063/1.2913201

Ultrafast transformation of graphite to diamond: An ab initio study of graphite under shock compression

Christopher J. Mundy, Alessandro Curioni, Nir Goldman, I.-F. Will Kuo, Evan J. Reed, Laurence E. Fried, and Marcella Ianuzzi

Citation: The Journal of Chemical Physics **128**, 184701 (2008); doi: 10.1063/1.2913201
View online: http://dx.doi.org/10.1063/1.2913201
View Table of Contents: http://aip.scitation.org/toc/jcp/128/18
Published by the American Institute of Physics

Ultrafast transformation of graphite to diamond: An *ab initio* study of graphite under shock compression

Christopher J. Mundy,[1,a)] Alessandro Curioni,[2] Nir Goldman,[3] I.-F. Will Kuo,[3] Evan J. Reed,[3] Laurence E. Fried,[3] and Marcella Ianuzzi[4]
[1]*Chemical and Materials Science Division, Pacific Northwest National Laboratory, Richland, Washington 99352, USA*
[2]*IBM Research, Zurich Research Laboratory, CH-8803 Ruesschlikon, Switzerland*
[3]*Chemistry, Materials, Earth and Life Sciences, Lawrence Livermore National Laboratory, Livermore, California 94550, USA*
[4]*Paul Scherrer Institut, Winterthurerstrasse 190, CH-5232 PSI, Villigen, Switzerland*

(Received 16 November 2007; accepted 1 April 2008; published online 8 May 2008)

We report herein *ab initio* molecular dynamics simulations of graphite under shock compression in conjunction with the multiscale shock technique. Our simulations reveal that a novel short-lived layered diamond intermediate is formed within a few hundred of femtoseconds upon shock loading at a shock velocity of 12 km/s (longitudinal stress $>$ 130 GPa), followed by formation of cubic diamond. The layered diamond state differs from the experimentally observed hexagonal diamond intermediate found at lower pressures and previous hydrostatic calculations in that a rapid buckling of the graphitic planes produces a mixture of hexagonal and cubic diamond (layered diamond). Direct calculation of the x-ray absorption spectra in our simulations reveals that the electronic structure of the final state closely resembles that of compressed cubic diamond. © *2008 American Institute of Physics*. [DOI: 10.1063/1.2913201]

INTRODUCTION

Despite being an area of intense research, the phase boundaries and electronic properties of elemental carbon at extreme pressures and temperatures (e.g., 10–100 s of GPa and 1000 s of K) are relatively poorly known. Diamond anvil cell experiments have been used to study the transformations of graphite under static compression at extreme conditions of temperature and pressure.[1,2] Shock compression dynamically strains the sample in a uniaxial direction, while simultaneously heating the sample. Shock compression experiments can achieve nanosecond temporal resolution, and are thus well suited to study time-dependent phenomena. Shock compression experiments up to ~20 GPa have observed a martensitic phase transformation from graphite to diamond,[3] where the graphitic planes slide to form a hexagonal diamond, which, in turn, forms a cubic diamond. The transition from graphite to diamond was observed to occur in 10 ns for a 20 GPa shock. Shock Hugoniot parameters for graphite to diamond transitions have been measured up to 120 GPa using gas gun experiments.[4] (The Hugoniot is the locus of thermodynamic states accessible by a shock.) Laser-induced shock experiments have been used to study the melting curve of diamond to significantly higher pressure conditions (up to 2000 GPa).[5] However, experimental techniques have only recently been developed to perform *in situ* studies of chemical transformations in shocks.[6–8] Molecular and atomic scale information are difficult to experimentally obtain, and theoretical studies are necessary in order to develop simple chemical pictures for the high pressure-temperature behavior of the phase transformations of carbon.

A number of thermodynamic equilibrium simulations of carbon at extreme pressures and temperatures have been performed, where the pressure and temperature of the system are preset rather than simulating the numerous thermodynamic states induced by shock compression. Several studies have investigated the solid/liquid phase boundaries of carbon at high pressures and temperatures using both empirical[9,10] and *ab initio*[11,12] potentials. Relatively few studies have investigated the atomistic features of the martensitic phase transition of graphite to diamond. A previous density functional theory (DFT) study of hydrostatic constant pressure compression found that the sliding of graphite planes into an orthorhombic phase preceded the formation of diamond.[13,14] It has been postulated that a layered diamond phase could be formed by direct buckling of hexagonal graphite without plane sliding at pressures above 120 GPa.[13,14] It was concluded that the experimental observation of this phase was very unlikely. These studies differ from shock compression experiments in that the simulations are fixed at a single state point, whereas shock compression causes a material to visit numerous thermodynamic states. An additional key difference is that the stress in these simulations is hydrostatic, unlike shock waves, which contain regions of highly nonhydrostatic stress due to the uniaxial nature of planar shock compression.

Until recently, it has been extremely difficult to obtain a clear theoretical picture of chemistry behind shock fronts because direct simulation of shock compression can require tens of millions of particles.[15] One empirical potential has been developed for the study of shock-induced melting of diamond,[16] although the parametrization of such potentials

a)Electronic mail: chris.mundy@pnl.gov.

for high pressure carbon is still an active area of research.[9,10] In order to accurately model the breaking and forming of chemical bonds behind shock fronts, we are generally required to use DFT. Molecular dynamics (MD) calculations using DFT, however, are limited to only tens to hundreds of particles due to the extreme computational cost. This precludes making a direct one-to-one comparison between simulations and shock compression experiments, where the nonhydrostatic conditions present in the steady shock front can produce novel intermediate species and mechanisms. In particular, we are interested in determining a molecular level picture of the graphite to diamond phase transformation induced by shock loading. Thus, a computational capability to access both electronic states and information on chemical bonding, while capturing the nonhydrostatic nature of a steady shock and the concomitant MD, is necessary to elucidate chemical processes at extreme pressures and temperatures.

The multiscale shock technique[17–20] (MSST) is a simulation methodology based on the Navier–Stokes equations for compressible flow. Instead of simulating a shock wave within a large computational cell with many atoms,[15] the MSST computational cell follows a Lagrangian point through the shock wave as if the shock were passing over it. This is accomplished by time-evolving equations of motion for the atoms and volume of the computational of cell to constrain the stress in the propagation direction $\sigma_{xx} \equiv p$ to the Rayleigh line and the energy of the system to the Hugoniot energy condition.[17–19] In the case of a shock, conservation of mass, momentum, and energy across the shock front leads to the Hugoniot relation $E-E_0=\frac{1}{2}(p+p_0)(v_0-v)$, where E is the energy and v is the volume. A subscript 0 refers to the preshocked state, while quantities without subscripts refer to the postshocked state. The Rayleigh line $p-p_0=U^2\rho_0(1-\rho_0/\rho)$ (where U is the shock velocity and ρ is the density) describes the thermodynamic path connecting the initial state of the system to its final (Hugoniot) state. For a given shock speed, these two relations describe a steady planar shock wave within continuum theory. By constraining the MD system to obey these relations, MSST enables simulation of the shock wave with significantly fewer atoms and, consequently, with significantly smaller computational cost. MSST has been shown to accurately reproduce the sequence of thermodynamic states throughout the reaction zone of shock compressed explosives with analytical equations of state.[19] Linear scaling of computational work with simulation duration has enabled simulation lengths of up to 0.2 ns of tight-binding *ab initio* MD simulations of shock compressed nitromethane.[20]

In this study, we present large scale *ab initio* DFT MD simulations of the transformation of graphite to diamond under shock compression normal to the basal planes. We study significantly higher longitudinal shock stress than previous experiments.[3] We find that the martensitic phase transformation of graphite to diamond occurs much more rapidly as a result. We observe a novel mechanism for the phase transformation where the graphitic planes buckle directly, instead of sliding and forming an orthorhombic state first.[13,14] We identify this new intermediate as a layered diamond state, which is a mixture of hexagonal and cubic diamond. We then calculate the x-ray absorption spectra (XAS) of the various stages of our simulations and determine that the end state of the shock compression simulation has a diamondlike electronic configuration. Our results provide a detailed atomic picture from DFT of the chemistry behind shock fronts in graphite for the first time.

TABLE I. Table of simulation parameters and final thermodynamic states three calculations performed with different number of atoms (N) utilizing the Tersoff potential (Ref. 30) for carbon in conjunction with the MSST at a shock speed of 12 km/s. The initial densities were identical to those performed with DFT interaction potentials. All three simulations were run for 100 ps with a time step of 0.1 fs.

	$N=360$	$N=2880$	$N=23\,040$
T_{final} (K)	4918	4981	4978
P_{xx} (GPa)	130	130	130
ρ_{final} (g/cc)	3.5	3.6	3.6

SIMULATION DETAILS

We have used Car–Parrinello (CP) and Born–Oppenheimer (BO) MD in conjunction with MSST to ensure accurate simulation of the shock induced thermodynamic states. We employed an optimized version of the CPMD code[21,22] for the Blue Gene/L supercomputer at Lawrence Livermore National Laboratory. Four independent simulations using the CPMD software package[21] on 360 carbon atoms in conjunction with the MSST method were performed. We performed two Born–Oppenheimer ($BO_{1,2}$) calculations utilizing spin restricted DFT, and CPMD simulations[23] using both spin restricted and unrestricted DFT. A plane-wave cutoff of 120 Ry and the Perdew–Burke–Ernzerhof exchange and correlation functional[24] was used for the BO simulations, although a smaller cutoff of 90 Ry was found to converge the stress tensor and total energy for the CP simulations. Cutoffs were based on an uncompressed reference supercell. Subsequent shock compression yields a higher effective cutoff. We found the results for the spin unrestricted and spin restricted CP calculations to be nearly identical for both and consequently, only the spin restricted CP simulation is reported herein. The interaction between core and valence electrons are described by Martins–Troullier pseudopotentials.[25] An initial supercell (in cubic angstroms) of hexagonal graphite with size of $20.10\times12.75\times12.30$, corresponding to experimental graphite lattice parameters, was used in conjunction with Γ-point sampling of the Brillouin zone. All calculations were performed on four midplanes (4096 CPUs) of the Blue Gene/Light supercomputer at LLNL. To compute the XAS spectra, we have used the all-electron half-hole transition potential method with Gaussian and augmented plane-wave treatment of DFT as implemented in CP2K.[26,27] For this calculation, we have used a 6-311G** all-electron basis set for carbon.[28]

In order to investigate finite size effects, we have conducted MSST simulations using the classical potential for carbon from the work of Tersoff.[30] The resulting equations of state for system sizes of 360, 2880, and 23 040 carbon atoms

TABLE II. Simulation parameters and final thermodynamic states for all three simulations. An electronic mass of 25 a.u. was used for the CP runs. The EOS result is based on a fit to experiment (Refs. 4 and 29). The difference averages of sp^2 and sp^3 percentages for the BO_2 run is likely due to its short trajectory. Running averages of sp^2 and sp^3 fractions have been examined and indicate that trajectories from all simulations are converging to the same values.

	BO_1	BO_2	CP	EOS (Final state)
Cell mass (a.u.)	7×10^7	17×10^7	17×10^7	N/A
Time step (fs)	0.097	0.097	0.012	N/A
Wavefunction cutoff (Ry)	120	120	90	N/A
Wavefunction convergence Tolerance (a.u.)	5×10^{-5}	1×10^{-6}	N/A	N/A
T_{final} (K)	4084.2	4058.8	3351.2	5300
P_{xx} (GPa)	139.8	134.4	136.4	150
P_{tot} (GPa)	94.8	84.7	83.4	N/A
ρ_{final} (g/cc)	3.9	3.8	3.8	4.2
sp^2_{final} (%)	18	30	19	N/A
sp^3_{final} (%)	82	70	81	N/A

are shown in Table I. Given the insensitivity of the thermodynamic end states to system size using the Tersoff potential, system size effects are unlikely to be present in our DFT simulations. The MSST simulations with the Tersoff potential yielded an amorphous (e.g., noncrystalline) state upon shock compression, unlike the diamond phase obtained from DFT. Consequently, we have omitted discussion of its resulting structural parameters and molecular configurations.

RESULTS AND DISCUSSION

We chose a shock speed of 12 km/s in order to produce a shock strong enough to see plastic deformations, and see chemistry on computationally accessible time scales. Our simulations using shock velocities under 12 km/s did not yield a diamond phase on the time scale of the simulation (e.g., 5–10 ps). Simulation parameters for the DFT calculations and final thermodynamic states including equation of state (EOS) calculations[29] fit to experimental results are recorded in Table II. We achieved longitudinal stresses in the shock propagation direction of ~134–140 GPa in all three simulations. The total stresses (stress tensor trace) at the end of the simulations were 83–95 GPa. The nonhydrostatic stress tensor indicates that full plastic relaxation of stress to a hydrostatic state has not yet occurred after 1 ps of simulation and the simulation has not reached a final thermodynamic state. As a result of the Rayleigh line constraint and the high density of diamond relative to graphite, we expect the simulated pressures, temperatures, and densities to be below those of the EOS models in Table II which provide final shock states only. The time evolution of the thermodynamic properties of the shock compressed graphite simulation are shown in Fig. 1. After less than 200 fs, the simulations all experienced a rise in temperature and pressure followed by a plateau, and second rise plateau after an additional 100 fs. This is due to phase transformations and a rearranging of the chemical bonds of the system, discussed below.

Shock experiments performed on graphite up to 20 GPa have suggested that the transformation to the diamondlike

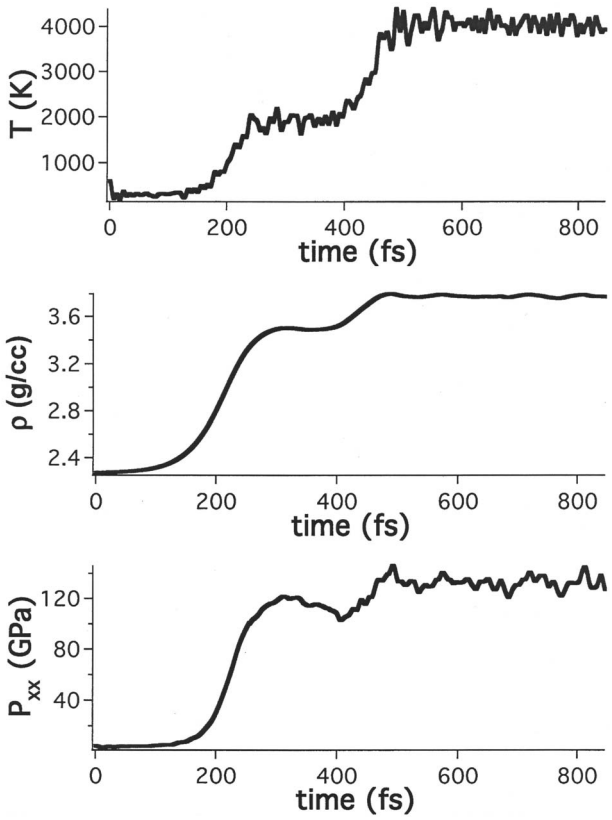

FIG. 1. Time evolution of the thermodynamic states induced by the 12 km/s shock velocity. The results are shown for the BO_2 simulation. The thermodynamic profiles of all three simulations were nearly identical.

state is martensitic[3] under the pressures studied, and occurs on a roughly nanosecond time scale. Our study, at 130 GPa, is close to the melting line of diamond. Thus, a change in mechanism to a nonmartensitic transformation with an amorphous intermediate is conceivable. An order parameter for tetrahedral configurations[31] provides insight into the time evolution of the graphite to a cubic diamond (perfectly tetrahedral state) phase transition. The order parameter contains an angular part and a distance part. The angular part S_g is defined as

$$S_g = \frac{3}{32}\sum_{j=1}^{3}\sum_{k=j+1}^{4}\left(\cos\psi_{j,k}+\frac{1}{3}\right)^2, \tag{1}$$

where $\psi_{j,k}$ is the angle subtended between the jth and kth bonds. The distance part of the order parameter is defined as

$$S_k = \frac{1}{3}\sum_{k=1}^{4}\frac{(r_k-\bar{r})^2}{4\bar{r}^2}, \tag{2}$$

where r_k is the radial distance from the central atom to the kth peripheral atom, $\bar{r}$ is the arithmetic mean of the four radial distances, and $\frac{1}{3}$ is a normalization factor. We considered the total value order parameter $S_{\text{tot}}=S_g+S_k$ here. For a random configuration of bonds (e.g., a liquid or amorphous solid), S_{tot} yields values of 0.25 or greater.[31] For diamond, the order parameter is 0. We computed the initial value of S_{tot} for graphite to be ~0.2. Consequently, we expect the value of S_{tot} to decrease monotonically if our simulations exhibit a martensitic phase transformation. A nonmartensitic phase

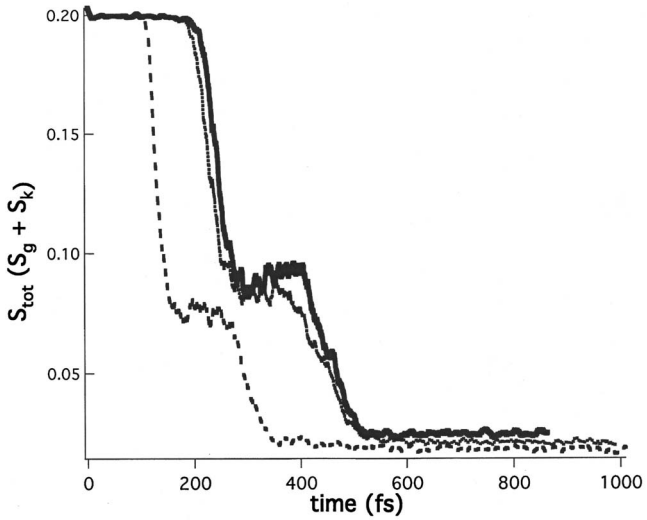

FIG. 2. Evolution of the tetrahedral order parameter as a function of time. The dashed curve corresponds to the BO_1 simulation and the solid curve to the BO_2 simulation. The dotted curve is the result from the CP simulation. The difference in the time scale to fully compress the simulation cell is dictated by the fictitious cell mass (see Table I). Graphite corresponds to a value of 0.2 and pure cubic diamond to a value of 0. A nonmartensitic transition to a liquid phase would have shown an increase in the value of the order parameter to 0.25 or greater, followed a monotonic decrease to 0.

transformation would exhibit an increase to a value equal to or greater than 0.25 if a liquidlike intermediate is formed first, followed by a decrease to 0.

Plots of S_{tot} for all three DFT simulations clearly show a martensitic phase transformation (Fig. 2). S_{tot} decreases rapidly and roughly monotonically to near-zero values as the graphite compresses to diamond. This indicates the absence of an amorphous intermediate state. The nonzero endpoints indicate that the final configurations are not perfectly tetrahedral. It is interesting to note the ~100 fs plateau observed for all three simulations, similar to Fig. 1. This is due to the transient layered diamond phase, which is discussed below. All three simulations yield extremely similar results for the structural variation as a function of time. Thus, the observed martensitic transformation is reproducible with different simulation protocols (see Table II). Our results suggest that the mechanism of the graphite to diamond remains martensitic between 20 and 130 GPa, although the time scale drops by three orders of magnitude. The CP simulation phase transformation is in good agreement with the BO simulations despite the electron heating issues in the CP simulation that cause the temperature to drift by ~180 K from the target (Hugoniot) energy and the BO simulation temperature.

In order to create a structural picture for the changes that occur during the shock compression, we have calculated the wide XAS (WAXS) (Fig. 3). The WAXS intensities $I(Q)$ are calculated using the following formula:[32]

$$I(Q) = \sum_{ij} f_C^2(Q)\exp(i\mathbf{Q}\cdot\mathbf{r_{ij}}), \tag{3}$$

where $f_C(Q)$ are the standard carbon atomic form factors.[33] We have used an x-ray energy of 37.45 keV for all calculations.[1] For the first few hundred femtoseconds of each simulation, the graphitic planes stay relatively intact, and we

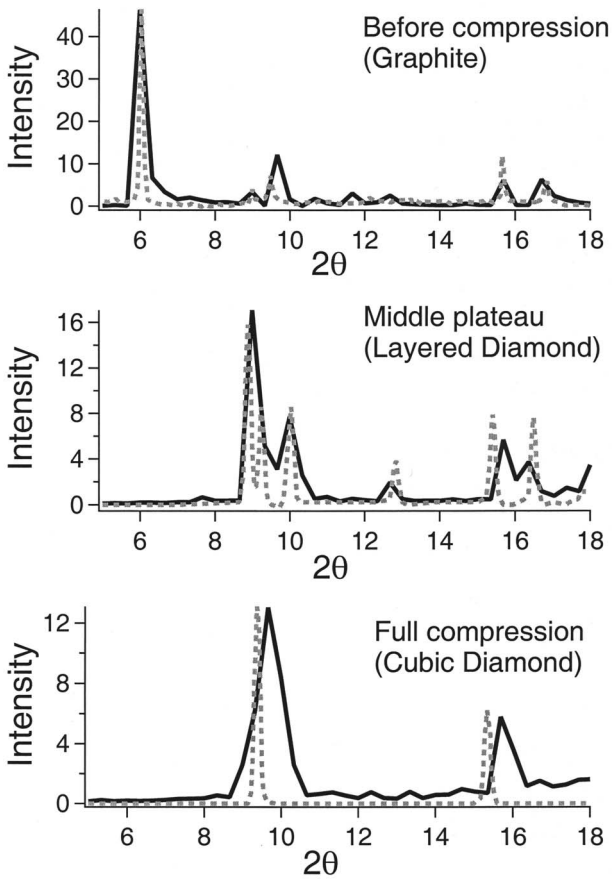

FIG. 3. Wide angle x-ray scattering intensities of the compressed states of graphite. All results shown are from BO_1 (black curves). The top panel (graphite) is averaged from zero to 300 fs, with comparison to experimental results (dotted curve) at 3 GPa (Ref. 1). The middle panel (layered diamond) is averaged from 300 to 500 fs, shown with comparison to simulations for hexagonal diamond (Ref. 14) (dotted curve). The missing doublet at ~9° and the coalescence of peaks at ~16° indicates a mixture of hexagonal and cubic diamond phases. The bottom panel (cubic diamond) is averaged over the remainder of the simulation, with comparison made to simulations at 20 GPa (Ref. 14) (dotted curve).

observed single peaks at ~6° and 9.5°, and a doublet centered at ~16°. This corresponds nearly exactly to experimental results for compressed graphite.[1] Comparison of the WAXS of the middle plateau of our simulations to that of hexagonal diamond[14] shows a mixture of hexagonal and cubic diamond spectra. Instead of a doublet at ~9°, we found a single peak, similar to what is found for cubic diamond. Our computed spectrum does exhibit the hexagonal diamond singlets at ~10° and 12.5°. However, the doublet found in hexagonal diamond at ~16° appears to be coalescing into the single peak found in cubic diamond. This mixed cubic/hexagonal diamond phase is similar to what is found in static simulations of graphite compressed to much lower conditions.[13] The graphite layers likely buckle after rapid compression, allowing for sp^3-sp^3 bonds to occur between the basal planes.[14] This represents a novel mechanism for the formation of cubic diamond from shock compression. The hexagonal diamond intermediate seen at lower shock velocities[3] is not observed under the strong shock loading studied here. In all three DFT simulations, the layered diamond phase transforms to cubic diamond within ~100 fs.

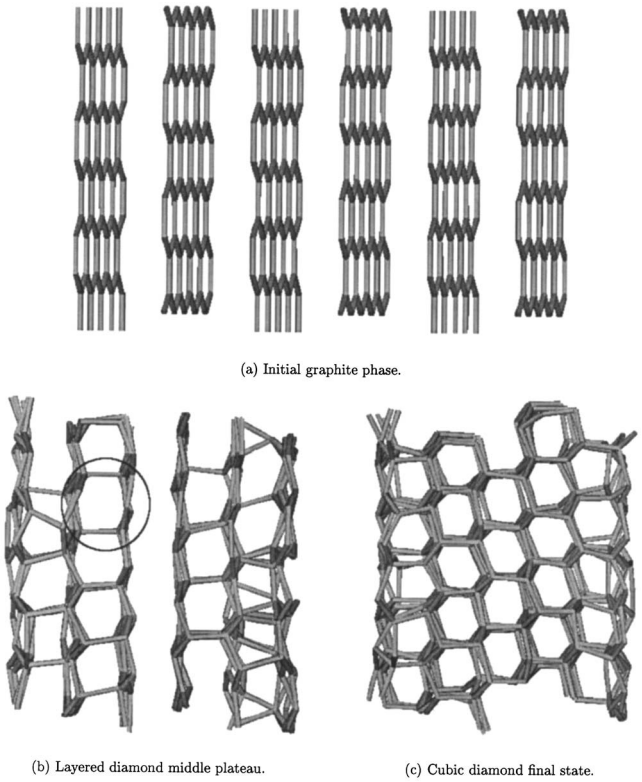

FIG. 4. Snapshots of the BO_1 simulation at various points during shock compression. The circled region in the layered diamond snapshot (b) corresponds to a likely hexagonal diamond region.

Snapshots of the three different phases found in our simulations (graphite, layered diamond, and cubic diamond) are shown in Fig. 4.

In addition to the above structural information, *ab initio* calculations also yield insight into the electronic states, which are not obtainable from empirical interaction potentials. In particular, we wish to investigate the effects of strong shock compression on the time evolution of the electronic structure of the system. Although the final state of our simulation appears to be structurally diamondlike, this does not guarantee the existence of a diamondlike (insulating) electronic configuration. Recent advances in the techniques for computing XAS from *ab initio* calculations using all-electron methods allow us to directly compute the spectroscopic signature of the final state achieved in our simulation. The XAS for our periodic supercell are shown in Fig. 5.

Our calculated XAS spectrum for graphite at 300 K (top panel) shows a near-edge feature at ~287 eV, which corresponds to a $1s$ to π^* transition, indicative of a π-bonding network.[1] The higher energy remainder of the spectrum corresponds to $1s$ to σ^* transitions (σ-bonding network). However, the XAS spectrum of the final state of our simulation (middle panel, black curve) has a marked the absence of the π^* transition and an enhanced σ^* part of the spectrum. This is expected for a σ bonded network structure such as cubic diamond. In addition, the spectrum exhibits a diffuse maximum at ~290–300 eV, a minimum at ~303 eV, and a second maximum at ~306 eV. The minimum at ~303 eV very closely corresponds to the experimentally measured "second band gap" signature of a diamondlike material.[34] For reference, we have computed the XAS of compressed cubic diamond in a hydrostatic state at the same density as our final compressed state (bottom panel). We observe that the position of the second band gap of the hydrostatically compressed cubic diamond is in good agreement with both experiment and the end state of our simulations.

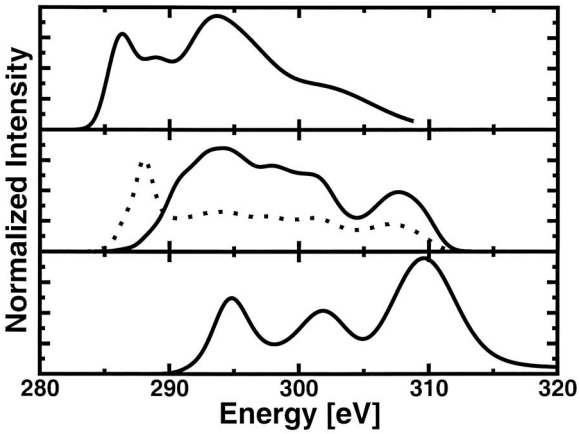

FIG. 5. Calculated XAS of (top panel) graphite at 300 K, (middle panel) our final compressed state, (bottom panel) hydrostatically compressed cubic diamond at the same density as the final compressed state. The XAS of graphite shows the π^* pre-edge intensity at ~285 eV and the σ^* intensity at ~295 eV. The middle panel shows the XAS spectrum averaged over 200 carbon centers. The dotted curve in the middle panel is the scaled partial XAS spectra of the sp^2-only carbon centers. This shows that the observed phase is more closely related to diamond than graphite.

In addition, we have also isolated the XAS of the simulation end state due to the sp^2-only carbon centers (middle panel, dashed curve). Due to the significantly lower concentration of sp^2-only sites (Table II), this normalized spectrum was then scaled by a factor of 0.6 in order to be visible on the same scale. The π^* signal of this compressed state is blueshifted relative to the π^* signal of the uncompressed graphite. This blueshift can be seen, although in a less dramatic, in the experiment[1] and is likely due to the effects of the pressure applied normal to the basal planes. We also observe a π^* transition at ~288 eV and a diminished σ-bonding network.

CONCLUSION

We have used *ab initio* MD to provide a simple atomistic picture for the shock-induced phase transformation of graphite to diamond. Our results indicate that the transition is martensitic at 130 GPa, which is consistent with experiments at 20 GPa.[3] This suggests that the mechanism may remain martensitic from 20 to 130 GPa along the shock Hugoniot. However, we note two significant differences in our findings. First, we find that the graphite to diamond transition occurs four orders of magnitude faster at 130 GPa than at the experimental pressure of 20 GPa (1 ps versus 10 ns). Second, we observe a completely different transformation mechanism than found in hydrostatic (not shock) simulations. We find that a new intermediate layered diamond phase is formed without plane sliding, through buckling of the basal planes. From examination of Table II, it is clear that the plastic relaxation of stress is not complete at the final simulation time

of 1 ps even though the phase transition to diamond is nearly complete at this time. Our computed XAS spectra indicate that the end state of our simulation contains an electronic signature of cubic diamond. However, due to the elevated temperatures and pressures compared to the experiment,[1] the features of our spectrum are likely broadened. In addition, calculation of the spectrum from sp^2-only sites in the system indicate trace amounts of π-bonds.

ACKNOWLEDGMENTS

This work was performed under the auspices of the U.S. Department of Energy by University of California LLNL under Contract No. W-7405-Eng-48. We would like to thank Tony Van Buuren, Trevor Willey, Dave Erskine, Jon Eggert, and Juerg Hutter for illuminating discussions. We also gratefully acknowledge Mike McCoy and Dale Nielsen of the Center for Applied Scientific Computing for generous travel funds for A.C. and for supporting this research.

[1] W. L. Mao, H. K. Mao, P. J. Eng, P. T. Trainor, M. Newville, C. C. Kao, D. L. Heinz, J. Shu, Y. Meng, and R. J. Hemley, Science **302**, 425 (2003).
[2] F. Bundy, W. Bassett, M. Weathers, R. Hemley, H. Mao, and A. Goncharov, Carbon **34**, 141 (1996).
[3] D. J. Erskine and W. J. Nellis, Nature (London) **349**, 317 (1991); J. Appl. Phys. **71**, 4882 (1992).
[4] W. H. Gust, Phys. Rev. B **22**, 4744 (1980).
[5] S. Brygoo, E. Henry, P. Loubeyre, J. Eggert, M. Koenig, B. Loupias, A. Benuzzi-Mounaix, and M. L. Gloahec, Nat. Mater. **6**, 274 (2007).
[6] Y. M. Gupta, Y. A. Gruzdkov, and G. I. Pangilinan, Chem. Phys. Lett. **283**, 251 (1998).
[7] M. D. Knudson, K. A. Zimmerman, and Y. M. Gupta, Rev. Sci. Instrum. **70**, 1743 (1999).
[8] P. A. Rigg and Y. M. Gupta, J. Appl. Phys. **93**, 3291 (2003).
[9] L. M. Ghiringhelli, J. H. Los, E. J. Meijer, A. Fasolino, and D. Frenkel, Phys. Rev. B **69**, 100101 (2004).
[10] L. M. Ghiringhelli, J. H. Los, E. J. Meijer, A. Fasolino, and D. Frenkel, Phys. Rev. Lett. **94**, 145701 (2005).
[11] A. Sorkin, J. Alder, and R. Kalish, Phys. Rev. B **74**, 064115 (2006).
[12] A. A. Correa, S. A. Bonev, and G. Galli, Proc. Natl. Acad. Sci. U.S.A. **103**, 1204 (2006).
[13] S. Scandolo, M. Bernasconi, G. L. Chiarotti, P. Focher, and E. Tosatti, Phys. Rev. Lett. **74**, 4015 (1995).
[14] F. J. Ribeiro, P. Tangney, S. G. Louie, and M. L. Cohen, Phys. Rev. B **72**, 214109 (2005).
[15] K. Kadau, T. C. Germann, P. S. Lomdhal, and B. L. Holian, Science **296**, 1681 (2002).
[16] S. V. Zybin, M. L. Elert, and C. T. White, Phys. Rev. B **66**, 220102 (2002).
[17] E. J. Reed, L. E. Fried, and J. D. Joannopoulos, Phys. Rev. Lett. **90**, 235503 (2003).
[18] E. Reed, L. E. Fried, M. R. Manaa, and J. D. Joannopoulos, in *Chemistry at Extreme Conditions*, edited by M. Manaa (Elsevier, New York, 2005).
[19] E. J. Reed, L. E. Fried, W. D. Henshaw, and C. M. Tarver, Phys. Rev. E **74**, 056706 (2006).
[20] E. J. Reed, M. R. Manaa, L. E. Fried, K. R. Glaesemann, and J. D. Joannopoulos, Nature Physics **4**, 72 (2008).
[21] CPMD code, Version 3.11.1, Copyright IBM Corp 1990–2006, Copyright MPI für Festkörperforschung Stuttgart, 1997–2001.
[22] J. Hutter and A. Curioni, ChemPhysChem **6**, 1788 (2005).
[23] R. Car and M. Parrinello, Phys. Rev. Lett. **55**, 2471 (1985).
[24] J. P. Perdew, K. Burke, and M. Ernzerhof, Phys. Rev. Lett. **77**, 3865 (1996).
[25] N. Troullier and J. L. Martins, Phys. Rev. B **43**, 1993 (1991).
[26] M. Ianuzzi and J. Hutter, Phys. Chem. Chem. Phys. **9**, 1599 (2007).
[27] CP2K code (http://www.cpk2.berlios.de, Copyright CP2K developers group, 2000–2006.
[28] W. J. Hehre, R. Ditchfield, and J. A. Pople, J. Chem. Phys. **56**, 2257 (1972).
[29] L. Fried and W. M. Howard, Phys. Rev. B **61**, 8734 (2000).
[30] J. Tersoff, Phys. Rev. Lett. **61**, 2879 (1988).
[31] P. L. Chau and A. J. Hardwick, Mol. Phys. **93**, 511 (1998).
[32] B. E. Warren, *X-Ray Diffraction* (Dover, New York, 1990).
[33] *International Table for X-Ray Crystallography*, edited by J. A. Ibers and W. C. Hamilton, 3rd ed. (Kluwer, Dordrecht, 1989), Vol. 3.
[34] F. L. Coffman, R. Cao, P. A. Pianetta, S. Kapoor, M. Kelly, and L. J. Terminello, Appl. Phys. Lett. **69**, 568 (1996).